Slow dynamics of stress and strain relaxation in randomly crumpled elasto-plastic sheets

Alexander S. Balankin, Orlando Susarrey Huerta, Francisco Hernández Méndez, and Julián Patiño Ortiz
Grupo "Mecánica Fractal," Instituto Politécnico Nacional, México Distrito Federal, Mexico 07738
(Received 23 March 2011; revised manuscript received 9 June 2011; published 9 August 2011)

Stress and strain relaxation in randomly folded paper sheets under axial compression is studied both experimentally and theoretically. Equations providing the best fit to the experimental data are found. Our findings suggest that, in an axially compressed ball folded from an elastic or elasto-plastic material, the relaxation dynamics is ruled by activated processes of an energy foci rearrangement in the crumpling network. The dynamics of relaxation is discussed within a framework of Edwards's statistical mechanics. The functional forms of the activation barrier between admissible jammed folding configurations of the crumpling network under axial compression are derived. It is shown that relaxation kinetics can be mapped to activated dynamics of depinning and creep of elastic interface in a disordered medium.

DOI: 10.1103/PhysRevE.84.021118 PACS number(s): 05.70.Ln, 68.60.Bs, 46.32.+x, 89.75.Fb

I. INTRODUCTION

Recently, there has been much interest in crumpling under the external loading of different kinds of thin materials, ranging from the microscopic level—graphene membranes to the macroscopic level—hand-folded paper and fault-related geological formations [1–8]. The relevant property that all thin materials share is that their stretching rigidity is much more than the bending rigidity. Consequently, the forced crumpling of thin matter provides a particularly clean and simple form of stress focusing [9] because the elastic energy is concentrated principally in the crumpling creases (ridges) joining adjacent vertex points of maximal curvature [10–14]. But perhaps the most salient feature of randomly crumpled matter is its behavior under external loads—folded materials offer a low resistance to axial compression [15–17], whereas, their resistance to hydrostatic compression is anomalously high [4,12,18].

The mechanical response of a crumpled sheet on an external force is determined by the crumpling network [2,4,12], [15–19]. The jammed configurations of a crumpling network in randomly folded matter can evolve under an external driving force. This evolution involves movements of ridges and vertices and leads to the rearrangement of energy foci [20–22]. Statistical mechanics and thermodynamics of soft jammed systems in inherent states can be treated within a framework of the Edwards approach to the statistical mechanics description of granular materials [23]. The proposal of Edwards may be summarized as follows: Given a certain configuration attained dynamically, physical observables are obtained by averaging over the usual equilibrium distribution at the corresponding volume, energy, etc., but restricting the sum to the jammed configuration or inherent states defined as the stable configurations in the potential energy landscape. The strong ergodic hypothesis that all jammed configurations of a given volume can be taken to have equal statistical probabilities leads to the definition of configurational entropy S as the logarithm of the number of jammed configurations (Ω) of a given volume (V) and an energy of jammed configuration (E), etc. [23]. Associated with configurational entropy are the state variables, such as compactivity $\Psi^{-1} = (\partial S/\partial V)_E$ and configurational temperature,

$$T_{\rm conf}^{-1} = (\partial S/\partial E)_V \,, \qquad (1)$$

which play the role of effective temperature in statistical mechanics of frozen systems in inherent states (see Refs. [23–25]). In general, Ψ and $T_{\rm conf}$ are independent variables. Specifically, the configurational temperature determines the energy fluctuations in the system, while compactivity governs the volume fluctuations.

Following the original ideas developed by Edwards and Oakeshott [23], in a previous paper [16], we have suggested that mechanical properties of randomly crumpled thin matter can be understood within a framework of Edwards's thermodynamics of the crumpling network. Generally, in this way, the mechanical response of a randomly crumpled sheet on external loads is determined by the volume and shape dependences of the free energy of the crumpling network [16]. In particular, the mechanical behavior of the randomly folded sheet in a thee-dimensional stress state is dominated by the volume dependence of the crumpling network enthalpy, whereas, the response of the crumpling network to axial compression is controlled by the shape dependence of network entropy [16].

Accordingly, under increasing hydrostatic pressure, the diameter (R) of a ball, folded from a thin sheet, decreases as $R \propto P^{-\alpha}$, where the scaling exponent α is expected to be universal for elastic sheets [26], whereas, in the cases of elasto-plastic and plastic sheets, the value of α is dependent on the energy dissipation in crumpling creases [18,27,28]. Besides, at a fixed pressure (P = const), the diameter of a ball folded from an elasto-plastic or predominantly plastic sheet decreases logarithmically in time for periods of up to several hours [18]. Furthermore, once the folding force is withdrawn, the diameter of the ball, folded from the elasto-plastic sheet, increases logarithmically in time for periods of up to several days [29]. In contrast to this, a ball folded from a predominantly plastic material, such as aluminum foil, does not swell in size after the folding force is withdrawn [30] because of an insufficient amount of elastic energy stored in the crumpling creases.

Under increasing axial compressive force, the mechanical behavior of a ball folded from an elastic or elasto-plastic sheet with free-lateral dimensions is governed by the shape dependence of the crumpling network entropy [16]. In this way, it was demonstrated that the applied force F is related to

the compression ratio $\lambda = H/R$ as

$$F = K_0\left(\frac{1-c}{\lambda - c} - 1\right), \tag{2}$$

where K_0 is the ball stiffness, R is the ball diameter before compression, $H = R - u$ is the ball height in the direction of compression (see the insets in Fig. 3 of Ref. [16]), u is the corresponding displacement, and $c = nh/R$ is the minimal compression ratio, while nh is the minimal possible thickness of the folded sheet of the initial diameter R under axial compression (h is the sheet thickness, and n is the number of incompressible layers) [16]. Moreover, it was shown that the axial stiffness of the randomly crumpled sheet is a linear function of configurational temperature defined by Eq. (1), i.e.,

$$K_0 = \kappa_0 T_{\mathrm{conf}}, \tag{3}$$

where κ_0 is a function of the thickness and mechanical properties of paper [16].

If lateral dimensions of the test specimen, folded from thin sheets, are free of any confinement, an axial compression of the specimen is accompanied by its lateral expansion. It has been found experimentally that the lateral expansion ratio $\lambda_\perp = R_\perp/R$ is related to the axial compression ratio as $\lambda_\perp = \lambda^{-\nu}$, where $R_\perp$ is the specimen size in the plane perpendicular to the compression direction, while ν is the Poisson index [17]. Conversely, when the lateral dimensions of the crumpled sheet are confined, the sheet resistance to the axial compression is dominated by the volume dependence of the crumpling network enthalpy such that, when compressive force F_0 is applied, an instant compression ratio λ_0 is related to F_0 according to the power law relation $\lambda_0 \propto F_0^{\alpha_1}$, where $\alpha_1 = 3\alpha/(1+2\alpha)$ [4,26].

Under a constant axial compressive force $F_0 = \mathrm{const}$, the size H of a ball folded from an elasto-plastic sheet slowly decreases [4,19] (in some experiments, this creep deformation was observed for several weeks, after which the crumpled sheet had not yet reached its minimum height [4]). The dependence of H on time is not continuous but rather is interrupted by sudden changes, which can be attributed to sudden ridge collapses [19]. Even so, it was found that the overall change in the ball height $\Delta H(t) = H(0) - H = R\,[\lambda(0) - \lambda]$ can reasonably be fitted by a simple relation of the form

$$\lambda = a - \mu \ln(t/s), \tag{4}$$

where a and μ are fitting parameters [4,19]. It should be pointed out that logarithmic behavior (4) was observed in experiments with free lateral dimensions (see Ref. [19]) as well as when the lateral dimensions of the axially compressed specimen were confined (see Ref. [4]). It is also pertinent to note that logarithmic creep was observed in many elasto-plastic materials [31–34] and is commonly associated with an Arrhenius-like relaxation kinetics [35], while the effective temperature, which accounts for temporal fluctuations, can be of thermal or nonthermal nature (see Refs. [4,36–40]).

On the other hand, if a crumpled sheet is axially compressed up to a compression ratio, which is further held constant ($\lambda = \mathrm{const}$), the compressive force slowly decreases in time. Albuquerque and Gomes [41] demonstrated that, under a constant compression ratio, the relaxation of compressive force applied to hand-folded aluminum foil can be well fitted with the stretched exponential function,

$$F = F_0 \exp\left[-\left(\frac{t}{\tau_0}\right)^{\eta}\right], \tag{5}$$

where η and τ_0 are fitting parameters. Furthermore, the exponent $\eta = 0.28 \pm 0.03$ was suggested to be universal, while the experimental values were varied in the range from 0.24 to 0.4 [41]. However, numerical simulations performed in Ref. [42] suggest that η should be a function of the fractal dimension of the folded sheet.

To summarize, the forms and mechanisms of slow stress and strain relaxation in randomly folded matter under external forces still are not understood well. Specifically, while the axial deformation (creep) of a folded ball under a constant force displays logarithmic decay (2) within a wide range of time, a strong deviation from logarithmic behavior is observed for the early times [19]. Furthermore, the force relaxation (5) was studied only in axially compressed predominantly plastic aluminum foils [41], the mechanical behavior of which differs from that of balls folded from elasto-plastic sheets, such as a paper (see Refs. [17,28]). The relaxation of compressive force in specimens folded from crumpled papers has not been tested.

Accordingly, the purpose of this paper is to clarify the mechanisms and functional forms of stress and strain relaxation in hand crumpled elasto-plastic sheets subjected to axial compression. This paper is organized as follows. In Sec. II, we describe the details of experiments performed in this paper. Experimental results and their best empirical fittings are reported in Sec. III. Section IV is devoted to the discussion of experimental findings. Phenomenological equations, describing the stress and strain relaxation, are derived, and their physical interpretation is discussed. A brief summary of the main findings and conclusions are given in Sec. V.

II. EXPERIMENTAL DETAILS

In this work, the experiments were performed with hand-folded sheets of Kraft (thickness of $h = 0.141$ mm) and Biblia (thickness of $h = 0.039$ mm) papers. Square sheets with edge sizes of $L = 100$, 200, 400, and 600 mm were hand crumpled into approximately spherical balls. At least 6 balls were folded from sheets of each size of Kraft paper, and 15 balls were folded from sheets of the size of $L = 400$ mm of Biblia paper. Once the folding force is withdrawn, the ball diameter increases with time for approximately 6–8 days due to the strain relaxation in the folding creases (see Ref. [29]). Therefore, all experiments reported below were performed at least 10 days after a sheet was folded.

Paper is a composite visco-elasto-plastic material [43]. Paper properties are sensitive to variations in paper moisture and temperature, which are strongly dependent on ambient temperature and humidity [34,43]. Accordingly, in this work, the ambient temperature and humidity were monitored continuously during each experiment. Furthermore, some force and strain relaxation experiments had been carried out in a climatic chamber with controlled temperature (variations are less than 1°C) and relative humidity (variations are less than 3%).

Two series of experiments were performed with balls folded from paper sheets. In the first series of experiments, folded balls were tested under a constant axial compression rate. Test specimens were compressed with a loading rate of 2 mm/s using a universal test machine MTS-858-5. Figure 1(a) shows the force-compression behavior of a randomly folded paper ball under axial compression. Under the increasing compression force, the compression ratio λ follows relation (2) [see Fig. 1(a)], which can be rewritten in the form $F = K_0\varepsilon_e$, where $\varepsilon_e = u/H_e$ is the effective strain, while

$$H_e = H - nh = (R - nh) - u \tag{6}$$

is the effective ball size in the direction of compression [see Fig. 1(b)].

Once the compression is suddenly stopped at a fixed compression ratio $\lambda = \lambda_{F1}$, which is further held constant, the compressive force decreases in time, as shown in Fig. 1(c). When, after several hours of relaxation, the compression is reinitiated, the compressive force quickly increases as λ is decreased up to λ_{F2} [see the inset in Fig. 1(a)] such that, for compression ratios $\lambda \geqslant \lambda_{F2}$, the force-compression curve follows the same relation (2) as before relaxation [see Figs. 1(a) and 1(b)]. Furthermore, during unloading at the rate of 2 mm/s, the force-compression curve goes downward up to $F(\lambda_R) = 0$, where λ_R is the remanent compression ratio [see Fig. 1(a)], the value of which depends on the loading and unloading rates as well as on the time of compressive force relaxation under the constant compression ratio of $\lambda = \lambda_{F1}$. Once the compression force is withdrawn, λ slowly (and almost logarithmically) increases with time of approximately 1 week.

It should be pointed out that the force-compression relation (2) cannot be presented in terms of apparent stress ($\sigma = F/A_\lambda$) and effective strains because the area of loading (A_λ) is ill defined during the axial compression test as well as during ball compression under a constant force. Moreover, the distributions of stress and strains within an axially compressed ball are essentially inhomogeneous. However, we noted that, during stress relaxation under a constant deformation ratio ($\lambda = \lambda_0 = \text{const}$), a change in the apparent loading area was less than 2%. Hence, one can assume that, in this case, the equality,

$$\frac{\sigma(\lambda_0,t)}{\sigma_0(\lambda_0)} = \frac{F(\lambda_0,t)}{F_0(\lambda_0)} \tag{7}$$

holds with acceptable accuracy. Notice that equality (7) was already employed in Ref. [41]. Nevertheless, in this paper, experimental data and their fittings are given using the compressive force as the primary experimental attribute.

Figure 2 shows the graph of compressive force relaxation in a paper ball under a constant compression ratio together with graphs of air temperature (T) and humidity (W_H) obtained in an experiment carried out in a climatic chamber. One can see that abrupt changes in air humidity and temperature are accompanied by changes in compressive force behavior. We also noted that slow but large variations of T or/and W_H also affect the force relaxation behavior. Accordingly, the experimental data reported below were obtained either in experiments carried out in a climatic chamber with controlled air temperature and humidity or in an ambient air environment, when the variations in air temperature and humidity, during the experiment, were less than 2 °C and 5%, respectively. If, during a relaxation test, a change in temperature or humidity was greater, only the data of the initial time interval (during which $\Delta T \leqslant 1$°C and $\Delta W_H \leqslant 0.1 W_H$) were analyzed.

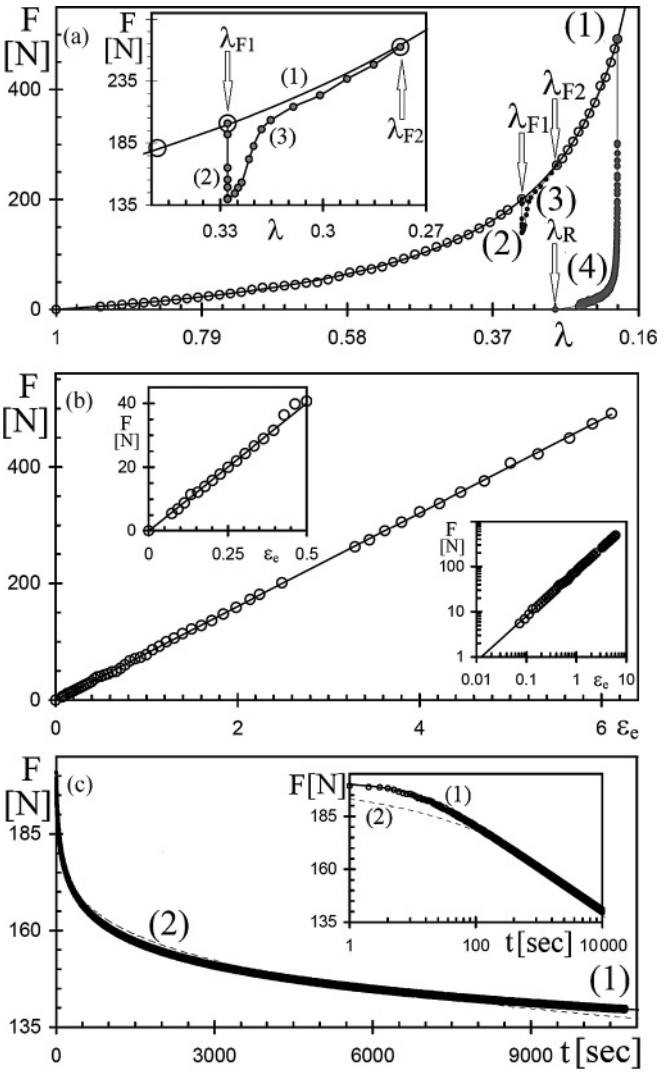

FIG. 1. (a) The force - compression curve of the ball folded from a square sheet of Kraft paper with an edge size of $L = 400$ mm under axial compression with the rate of 2 mm/s: circles, experimental data; curve 1, data fitting with Eq. (2); curve 2 corresponds to the compressive force relaxation shown in panel (c); curve 3, the transient regime in the range of the compression ratio of $\lambda_{F1} = 0.2775 \leqslant \lambda \leqslant \lambda_{F2} = 0.3279$, which is shown in more detail in the inset; and curve 4, unloading with the rate of 2 mm/s. (b) The force - effective strain curve obtained from the data presented in panel (a); the top inset shows the amplified initial part of $F(\varepsilon_e)$ behavior, while the bottom inset shows the log-log plot of F versus ε_e: straight lines, data fitting by Eq. (2) with $K_0 = 80.17$ N and $c = 0.058$. (c) Force relaxation at the fixed compression ratio of $\lambda_{F1} = 0.3279$; the inset shows the semilogarithmic plot of the force relaxation. Circles, experimental data; solid curve 1, data fitting by Eq. (8) with $\tau_F = 10.92$ s and $\beta = 0.044$; dashed curve 2, data fitting with the stretched exponential function (5) with $\tau_0 = 6.6$ days and $\eta = 0.245$.

Besides, in this paper, to have a more intimate reference to stress relaxation in balls folded from aluminum foil, we also

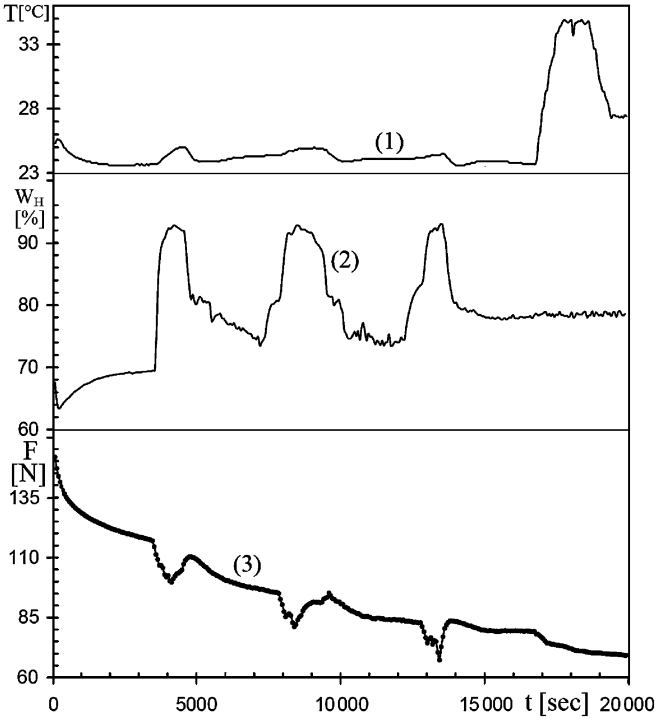

FIG. 2. Effects of abrupt changes in ambient temperature (curve 1) and humidity (curve 2) on the relaxation of the compressive force (curve 3) in the test of an axially compressed ball folded from a square sheet of Kraft paper with an edge size of $L = 400$ mm performed in a climatic chamber.

have performed three stress relaxation tests with balls with diameters of $R = 27$ mm folded from square sheets with edge sizes of $L = 240$ mm of aluminum foil with thicknesses of $h = 0.02$ mm.

In the second series of experiments, the folded balls were subjected to constant compressive forces $F_M = Mg$ supplied by a mass M, where g is the gravitational acceleration constant. The compressive weight was provided by metal plates with diameters of 16 cm placed horizontally on the top of the ball positioned inside of an acrylic tube with a diameter of 16.2 cm, which ensured that, at all times, the compressive weight was horizontal within a few degrees (see bottom inset in Fig. 3). Notice that, in our experiments, the diameters of balls tested were less that 10 cm such that the lateral sides of the balls were not subjected to any confinement. The ball height (distance between steel plates) was monitored with a laser micrometer MTS LX-500.

Once a weight M was placed on the ball, the ball almost instantly was compressed up to a compression ratio of $\lambda = \lambda_M$ such that $F_M = Mg$ and λ_M obeyed the relation (1). Thereupon, the compression ratio slowly decreased with time (see the top inset in Fig. 3) for more than 1 month [44].

In some experiments, after several hours of compression (t_1), the weight plate was suddenly trapped such that its position was fixed (using a rigid steel string attached to the weight plate) at $\lambda = \lambda_{t1} = \text{const}$ for a period of time $\Delta t = t_2 - t_1$ (see Fig. 3). It should be pointed out that, during this period ($\Delta t = t_2 - t_1$), the compressive force did not become zero, rather it slowly decreased in time in the same way as observed in the stress relaxation experiments at the constant

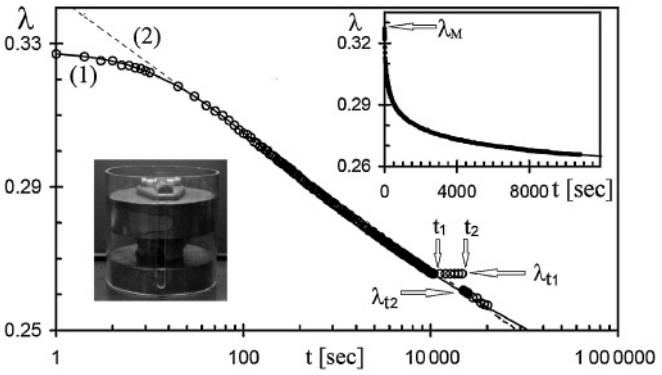

FIG. 3. Semilogarithmic graph of compression ratio λ versus time t for a ball folded from a square paper sheet of Kraft paper with an edge size of $L = 400$ mm subjected to constant compressive force. After the compressive force is supplied by mass $M = 20.718$ kg, the ball, almost instantaneously, is compressed up to $\lambda_M = 0.3279$ and then λ decreases with time up to the compression ratio $\lambda_{t1} = 0.2658$, at which the position of the plate is fixed for 3 h; when after $\Delta t = 3$ h, the plate is liberated, the ball, almost instantaneously, is compressed up to $\lambda_{t2} = 0.2611$; circles, experimental data; solid curve 1, data fitting by Eq. (9) with $c = 0.058$; $\tau_\lambda = 15.61$ s, and $\gamma = 0.068$; dashed line 2, data fitting by logarithmic equation (4) with $a = 0.3432$ and $\mu = 0.0082$; the top inset shows the graph of λ versus time excluding the data between t_1 and t_2, while the bottom inset shows the experimental setup.

compression ratio described above. When the plate was liberated again, the ball was compressed almost instantly up to λ_{t2}, and further compression followed the tendency observed before the compression was stopped (see Fig. 3). Notice that similar behavior was observed early in the experiments with crumpled Mylar sheets [45] reported in Ref. [4].

III. EXPERIMENTAL FINDINGS

The main aim of this paper is to find analytical expressions for the functions providing the best fits to the experimental data of force and effective strain relaxations. Accordingly, we have tried to fit the experimental data with many of the known forms of a relaxation function [46]. A comprehensive review of relaxation function forms can be found in Ref. [47]. The results of our efforts are reported below.

A. Compressive force relaxation under a fixed compression ratio

We found that the compressive force relaxation under a fixed compression ratio $\lambda = \lambda_F$ is best fitted with the following relationship:

$$F = F_0 \left[1 - \beta \ln \left(1 + \frac{t}{\tau_F} \right) \right], \tag{8}$$

where the force F_0 is related to λ_F according to relationship (2), while β and τ_F are fitting parameters [see Figs. 1(b) and 4]. Moreover, we found that fitting parameters are statistically independent of the sheet size, the ratio L/R, and the initial force $F_0(\lambda_F)$ [see the captions of Figs. 1(c), 4, and 5]. At the same time, we noted that τ_F was very sensitive to the paper properties, ambient humidity, and temperature during

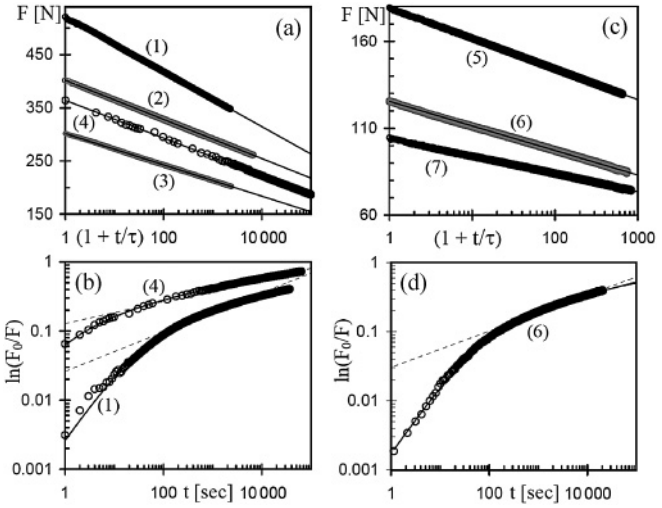

FIG. 4. Compressive force relaxation under the fixed compression ratios in balls folded from square sheets of (a) and (b) Kraft paper [$L = 600$ mm, $\lambda_M = 0.230(1)$, $L = 400$ mm, $\lambda_M = 0.148(2)$, $L = 200$ mm, $\lambda_M = 0.3(3)$, and $L = 100$ mm, $\lambda_M = 0.135(4)$] and (c) and (d) Biblia paper with $L = 300$ mm [$\lambda_M = 0.180(5)$, $\lambda_M = 0.185(6)$, and $\lambda_M = 0.265(7)$]. (a) and (c) Semilogarithmic graphs of F versus $1 + t/\tau$; (b) and (d) log-log graphs of $\ln(F_0/F)$ versus t . Circles, experimental data; solid lines, data fitting by Eq. (8) with $\beta = 0.043$ and $\tau_F = 15.99$ s. (1), $\beta = 0.0397$ and $\tau_F = 5.63$ s (2), $\beta = 0.0424$ and $\tau_F = 15.5$ s (3), $\beta = 0.0423$ and $\tau_F = 0.31$ s (4), $\beta = 0.0427$ and $\tau_F = 31.1$ s (5), $\beta = 0.0489$ and $\tau_F = 27.8$ s (6), $\beta = 0.043$ and $\tau_F = 24.4$ s (7); dashed lines, data fitting by the stretched exponential function (5) with $\eta = 0.28$ (1), 0.16 (4), and 0.26 (6).

the test, whereas, values of β, obtained in 16 force relaxation experiments with balls folded from two different papers, varied in a relatively narrow range of $0.39 \leqslant \beta \leqslant 0.49$ with the mean $\beta = 0.041 \pm 0.006$ (see Fig. 5). These findings suggest that characteristic time scale τ_F can be associated with the internal relaxation process and is determined by the paper properties that are strongly dependent on the paper moisture and temperature [48], whereas, β seems to be universal. However, a statistically small number of available experimental data are rather insufficient to affirm this universality.

We noted that force relaxation in axially compressed paper balls could not be fitted well with Eq. (5) [see Figs. 4(b) and 4(d)]. At the same time, we found that the compressive force relaxation in an axially compressed ball folded from aluminum foil seemed to more closely follow the stretched exponential function (5) suggested in Ref. [41] rather than Eq. (8) (see Fig. 6). This finding suggests that mechanisms of the compressive force relaxation in axially compressed balls folded from elasto-plastic paper sheets and from predominantly plastic aluminum foil are different. Notice that, previously, the role of plastic deformations in crumpling mechanics was discussed in Refs. [11,13,27,28].

B. Strain relaxation (creep) under a constant compressive force

In the case of creep deformation of a crumpled sheet under constant compressive force $F_M = Mg$, we found that

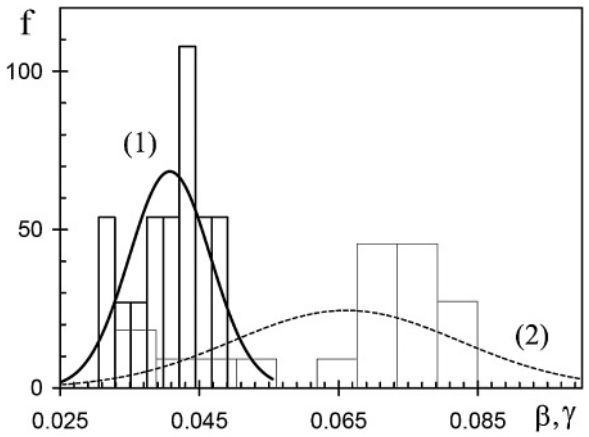

FIG. 5. Statistical distributions f of fitting parameters β (1) and γ (2) for balls folded from sheets of Kraft and Biblia papers in arbitrary units. Bins, experimental data; curves, data fitting by normal distributions with means $\overline{\beta} = 0.041(1)$ and $\overline{\gamma} = 0.066(2)$, respectively.

experimental data on the time dependence of the compression ratio are best fitted with an empirical relationship of the form

$$\lambda(t) = c + \frac{\lambda_M - c}{1 + (1 - \lambda_M)\gamma \ln(1 + t/\tau_\lambda)}, \tag{9}$$

where initial compression ratio $\lambda(0) = \lambda_M$ is related to $F_M = Mg$ according to the force-deformation relationship (2), while τ_λ and γ are fitting parameters (see Figs. 3, 7, and 8). Notice that coefficient $(1 - \lambda_M)$, before γ, assures that there is no creep without external compressive force ($M = 0$). We also found that values of γ, obtained in 19 experiments from two different papers, vary in a range of $0.033 \leqslant \gamma \leqslant 0.085$,

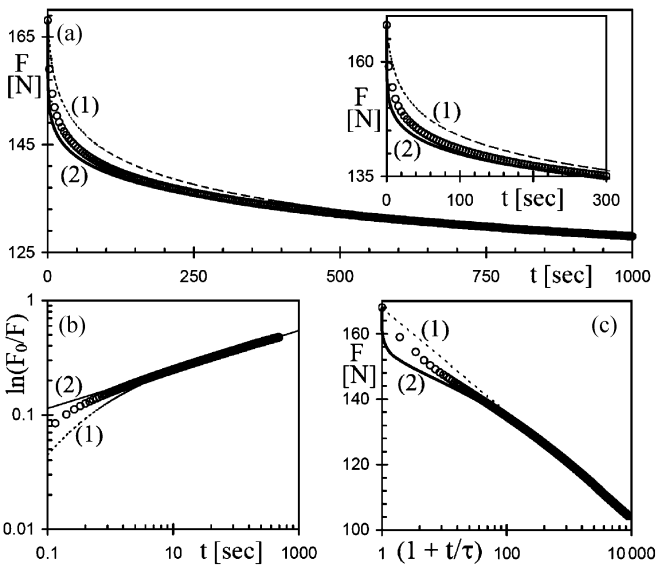

FIG. 6. Compressive force relaxation under a fixed compression ratio in a ball folded from aluminum foil: (a) graph of F versus t (inset shows the initial part of the same graph); (b) log-log graph of $\ln(F_0/F)$ versus t; (c) semilogarithmic graph of F versus $(1 + t/\tau)$, where $\tau_F = 3.25$ s. Circles, experimental data; dashed curves 1, data fitting by Eq. (8) with $\tau_F = 3.25$ s and $\beta = 0.0415$; solid curves 2, data fitting by Eq. (5) with $\eta = 0.17$ and $\tau_0 = 9.91$ h.

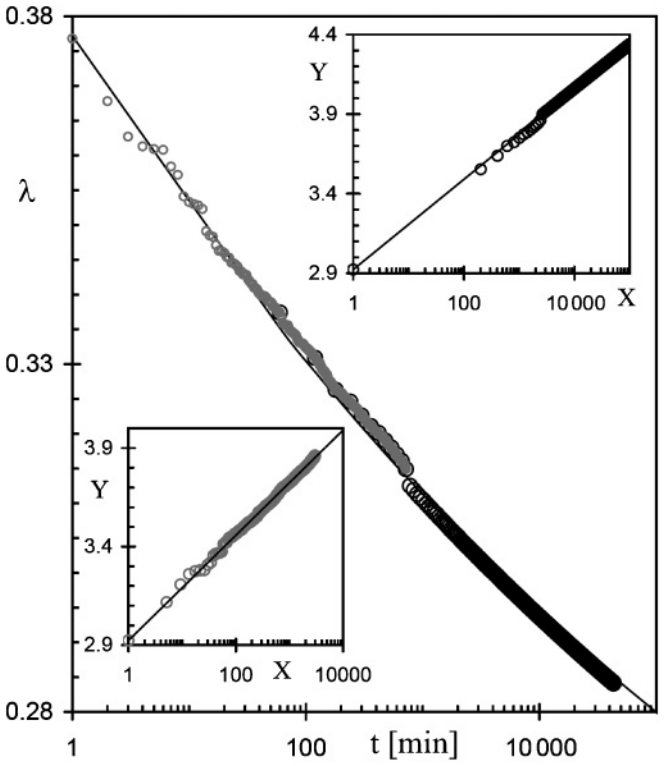

FIG. 7. Creep deformation of balls folded from square sheets with different edge sizes subjected to axial compressive force $F_M = Mg$. (a) Semilogarithmic graph of λ versus t for the ball folded from Kraft paper with the size of $L = 400$ mm under the weight of $M = 15.3$ kg: small gray circles, experimental data taken each minute for 12 h; large black circles, experimental data taken each hour for 30 days; solid line, data fitting by Eq. (9) with $c = 0.056$, $\tau_\lambda = 14.4$ s, and $\gamma = 0.076$. Insets show semilogarithmic graphs of $Y = 1/(\lambda - c)$ versus $X = 1 + t/\tau$ of data taken each minute for 12 h [bottom inset, data fitting by Eq. (9) with $c = 0.056$, $\tau_\lambda = 14.4$ s, and $\gamma = 0.065$] and each hour for 30 days [top inset, data fitting by Eq. (9) with $c = 0.056$, $\tau = 17.8$ s, and $\gamma = 0.07$].

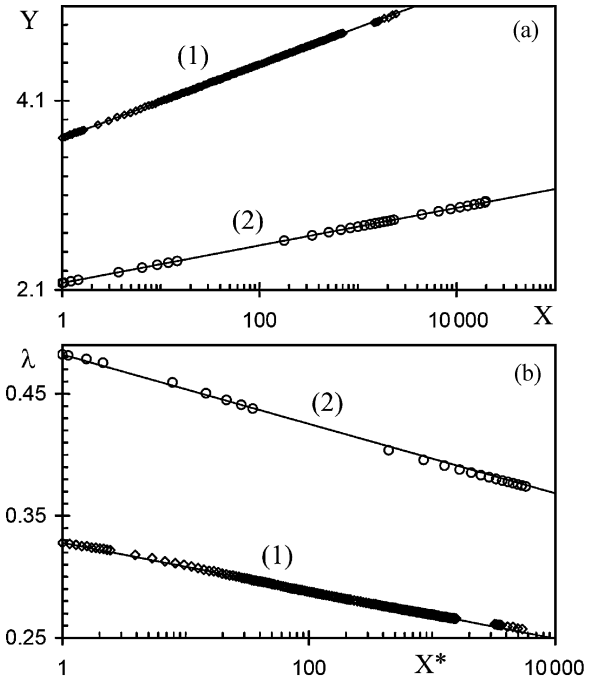

FIG. 8. Data fittings for the strain relaxation in axially compressed balls folded from Kraft paper with the size of $L = 400$ mm under the weight of $M = 20.718$ kg for 25.83 h (1) and Biblia paper with the size of $L = 300$ mm under the weight of $M = 5$ kg for 5 days (2): (a) semilogarithmic graphs of $Y = 1/(\lambda - c)$ versus $X = 1 + t/\tau$: symbols, experimental data; straight lines, data fitting by Eq. (9) with: $c = 0.058$, $\tau_\lambda = 15.3$ s, $\gamma = 0.069$ (line 1, squared correlation coefficient $R^2 = 0.9998$), and $c = 0.022$, $\tau_\lambda = 8.8$ s, and $\gamma = 0.077$ (line 2, $R^2 = 0.9999$); (b) semilogarithmic graphs of λ versus $X^* = 1 + t/\tau^*$: symbols, experimental data from panel (a); straight lines, data fitting by Eq. (10) with: $\lambda_M = 0.3279$, $\tau^* = 6.9$ s, $\mu^* = 0.0085$(curve 2, $R^2 = 0.9977$), and $\lambda_M = 0.4823$, $\tau^* = 8.8$ s, and $\mu^* = 0.0123$ (curve 2, $R^2 = 0.9974$).

which is considerably wider than the interval of β variations (see Fig. 5). Furthermore, while one may expect that the characteristic time scale τ_λ has the same nature as τ_F, we have no sufficient experimental data to support this assumption statistically because of the high sensitivity of τ_λ and τ_F to ambient conditions.

Here, it should be pointed out that, while the available experimental data for $t \gg \tau$ can be fitted well with Eq. (4), we found that, for any time interval, Eq. (9) provides a somewhat better fit than Eq. (4) (see Fig. 3) or its modification in the form

$$\lambda = \lambda_M - \mu^* \ln(1 + t/\tau_\lambda), \tag{10}$$

where μ^* and τ^* are fitting parameters (see Fig. 8). Notice also that, according to Eq. (9), the compression ratio is $\lambda \to c$ as $t/\tau \to \infty$, whereas, Eqs. (4) and (10) both suggest that the minimum possible compression ratio $\lambda = c$ can be achieved in a finite time $\tau_C \approx \tau_\lambda \exp[(\lambda_M - c)/\mu^*]$ on the order of several years. However, for times $t \ll \tau_C$, it is appropriate to note that Eq. (10) can be viewed as the two first terms of the series expansion of Eq. (9), and so $\mu^* = (\lambda_M - c)(1 - \lambda_M)\gamma$, while Eq. (4) is the asymptotic of Eq. (10) for times $t \gg \tau_\lambda \leqslant 1$ min, and so one expects that $\mu = \mu^*$ and $a = \lambda_M + \mu \ln(\tau_\lambda)$. In this way, Eq. (9) is consistent with the experimental results reported in Ref. [19].

IV. DISCUSSION

Creep and compressive force relaxation are inherent mechanical behaviors of crumpled matter under external loads. It seems reasonable to assume that both are different performances of the same physical processes. In this paper, we also assume that relation (2) can be extended to the case of time-dependent stiffness of the folded sheet under axial compression as

$$F = K_\varepsilon(t)\varepsilon_e, \quad \text{when} \quad \varepsilon_e = \text{const}, \tag{11}$$

while

$$\varepsilon_e = K_F^{-1}(t)F, \quad \text{when} \quad F = \text{const}, \tag{12}$$

where $K_\varepsilon(t)$ and $K_F(t)$ are the time-dependent stiffness at the constant compression ratio and at the constant compression force, respectively. If so, the compressive force relaxation at the fixed deformation ratio and the effective strain relaxation at the constant compression force both are controlled by the

time dependence of the ball stiffness. Specifically, Eqs. (8), (11), and (12) imply that

$$K_\varepsilon(t) = K_0\left[1 - \beta \ln\left(1 + \frac{t}{\tau_F}\right)\right], \tag{13}$$

while

$$K_F^{-1}(t) = K_0^{-1}\left[1 + \gamma(1-c)\ln\left(1 + \frac{t}{\tau_\lambda}\right)\right], \tag{14}$$

such that $K_\varepsilon(t)/K_F(t) \neq 1$, while $K_\varepsilon(0) = K_F(0) = K_0$. The difference in the time behavior of the ball stiffness at the constant compression ratio and at the constant compressive force can be attributed, at least partially, to different time behaviors of loading area A_λ, which almost holds constant during stress relaxation under a constant compression ratio [see Eq. (7)], whereas, A_λ is an increasing function of time during ball compression under the force $F = Mg$.

A. Evolution equations

From Eqs. (11) and (13), it immediately follows that, in an axially compressed ball folded from an elasto-plastic sheet, the compressive force relaxation at constant effective strain $\varepsilon_e = \varepsilon_0$ obeys the following evolution equation:

$$\left(\frac{dF}{dt}\right)_\varepsilon = \varepsilon_0\left(\frac{dK_\varepsilon}{dt}\right)_\varepsilon = -\frac{\beta F_0}{\tau_F}\exp\left(-\frac{F_0 - F}{\beta K_0 \varepsilon_0}\right), \tag{15}$$

where $F_0 = K_0\varepsilon_0$ and $F = K_\varepsilon\varepsilon_0$. Notice that by taking relation (7) into account, Eq. (15) can be rewritten in terms of apparent stresses in the form

$$d\sigma/dt = \beta(\sigma_0/\tau_\sigma)\exp\left[-(\sigma_0 - \sigma)/\beta\sigma_0\right],$$

which was widely used in the studies of shear and stain hardening in fcc metals [36–38] and band formation in plastic materials [36,38] and granular media [40].

On the other hand, Eqs. (12) and (14) imply that, under a constant axial compressive force ($F = Mg$), the creep deformation is governed by the following evolution equation:

$$\left(\frac{d\varepsilon_e}{dt}\right)_F = -\frac{Mg}{K_F^2}\left(\frac{dK_F}{dt}\right)_F = \frac{\gamma(1-c)}{\tau_\lambda}\varepsilon_M \exp\left[-\frac{K_0(\varepsilon_e - \varepsilon_M)}{\gamma(1-c)Mg}\right], \tag{16}$$

where $\varepsilon_M = u_M/(R^* - u_M) = (1-\lambda_M)/(\lambda_M - c)$ is the initial effective strain, while λ_M obeys the force-deformation relationship (2) with $F = Mg$.

At this point, it is appropriate to note that an exponential dependence of the relaxation rate on a driving force (equal to or smaller than its threshold value) is commonly associated with fluctuation controlled kinetics, while temporal fluctuations in the system can have a thermal or nonthermal nature (see, for example, Refs. [4,36–40]). The fluctuation controlled kinetics can be of thermodynamic or pure mechanical nature. However, in Sec. I, we already stated that the mechanical behavior of crumpled sheets can be understood within the framework of Edwards's statistical mechanics of a crumpling network (see Ref. [16]). Accordingly, below, the relaxation in the crumpled sheet is also discussed within the same framework.

B. Thermodynamics of relaxation processes

Equations (16) and (17) suggest that relaxation processes in a crumpled sheet, subjected to axial compression, are ruled by temporal fluctuations, which allows overcoming an activation barrier ΔU between jammed configurations of the crumpling network. The intensity of temporal fluctuations in the crumpling network is controlled by the configurational temperature (1). Accordingly, in the spirit of Edwards's statistical mechanics, one can expect that the axial compression of the randomly folded ball leads to the rearrangement of energy foci such that the activation barrier ΔU between admissible jammed configurations of the crumpling network is a function of compressive force and effective strain. Hence, the relaxation rates are expected to obey the Arrhenius-like relation,

$$\left(\frac{\partial F}{\partial t}\right)_{\varepsilon_e}, \quad \left(\frac{\partial \varepsilon_e}{\partial t}\right)_F \propto -\exp\left(-\frac{\Delta U}{kT_{\text{conf}}}\right), \tag{17}$$

where k is the constant analogous to the Boltzmann one (see Refs. [23,24]).

Taking relationship (3) into account, from the comparison of Eq. (17) with evolution equation (15), it follows that, in a ball under a constant compression ratio $\lambda_0 = (1 + c\varepsilon_0)/(1 + \varepsilon_0)$, the activation barrier between admissible folding configurations,

$$\Delta U_\lambda = \frac{k}{\beta\kappa_0\varepsilon_0}(F_0 - F) \tag{18}$$

increases as the compressive force decreases due to dissipation and/or redistribution of the deformationenergy,

$$E_0 = \int_0^{u_0} F du \tag{19}$$

supplied to the crumpling network during the ball compression from R to $H_0 = \lambda_0 R = R - u_0$.

In the case of balls folded from elastic sheets, deformation energy (19) is redistributed due to the rearrangement of energy foci in the crumpling network, including the redistribution of elastic energy between the crumpling creases as well as the buckling and/or disappearance of folds. In the case of elasto-plastic sheets, a part of deformation energy (19) dissipates due to plastic deformations in the crumpling creases. Accordingly, when the compressive force is withdrawn, the ball, which is folded from an elastic sheet, recuperates its initial size, which is determined by the initial restrictions [49] but not the initial shape (see Fig. 2 in Ref. [16]). In contrast to this, the ball, which is folded from an elasto-plastic material, resets in a state with remanent deformation $\lambda_R < 1$ (see Fig. 1(a) of this paper and Fig. 1 in Ref. [16]) after the compressive force is withdrawn.

On the other hand, from Eqs. (3), (12), (16), and (17), when compression ratio λ decreases under a constant compressive force $F = Mg$, it follows that the activation barrier between admissible folding configurations,

$$\Delta U_F = \frac{kK_0}{\gamma\kappa_0(1-c)}\left[\frac{\varepsilon_e}{\varepsilon_M} - 1\right] \tag{20}$$

increases as the compression ratio decreases due to the rearrangement of the energy foci in the crumpling network and/or the strain relaxation in the crumpling creases.

Furthermore, Eq. (20) can be rewritten in the following form:

$$\Delta U_F = \frac{K_0(1+\varepsilon_M)}{\gamma\kappa_0(1-c)\varepsilon_M}\left[\frac{\Pi_M}{\Omega}-1\right]^{-1} = \frac{kK_0}{\gamma\kappa_0(1-c)}\left(1+\frac{K_0}{Mg}\right)\left(\frac{\Omega}{\Delta\Pi}\right), \quad (21)$$

where

$$\Omega = Mg(u-u_M) \quad (22)$$

is the work of the gravitational force during creep displacement $u-u_M=\Delta u$, while $\Pi_M = Mg\,(R-nh-u_M)$ is the available potential energy of the weight plate before creep and so,

$$\Delta\Pi = \Pi_M - \Omega = Mg(R-nh-\Delta u) \quad (23)$$

is the available potential energy of the weight plate after creep displacement Δu.

Equations (21)–(23) suggest that, in the case of the ball folded from an elastic sheet, the energy supplied to the crumpling network by the work of the gravitational force during creep displacement (22) is dynamically distributed in the crumpling network in such a way that the strength of jammed folding configurations f_C increases, whereas, the available potential energy of the weight plate (23), playing the role of driving force f, decreases. As a result, the activation barrier increases with the creep displacement. Once the compressive force is withdrawn, the ball, which is folded from an elastic sheet, recuperates its initial size $H=R$, nonetheless, the ball shape, which is associated with a specific jammed configuration of the crumpling network, can differ from the ball shape before compression (see Fig. 2 in Ref. [16]) because there are many equivalent folding configurations for given experimental conditions. In the case of the balls folded from elasto-plastic sheets, a part of the energy, which is supplied by the work (22), dissipates due to plastic deformations in the crumpling creases. This manifests in the remanent deformation of the elasto-plastic sheet after unloading.

It is interesting to note that evolution equation (17), with the activation barrier that is defined by Eq. (21), takes the form of an equation for the creep velocity of an interface, which is driven in a disordered medium by a driving force f less than a pinning strength f_c [50],

$$v \propto \exp\left[-\frac{U_c}{kT_{\text{eff}}}\left(\frac{f_c}{f}\right)^{\chi}\right],$$

where U_c is the energy scale, T_{eff} is the effective temperature of the disordered medium, while χ is the creep exponent. Hence, the dynamics of relaxation in the crumpling network, which is subjected to axial compression, can be mapped into dynamics of depinning and creep motions of an elastic interface in a medium with quenched disorder. This mapping implies that the driving force of the creep motion is $f \propto (\Delta\Pi)^{1/\chi}$, while the pinning strength of the jammed folding configurations is $f_C \propto \Omega^{1/\chi}$. Further analysis is needed to derive an analytic expression for the creep exponent χ.

C. Remark

In balls that are folded from predominantly plastic sheets, such as aluminum foil, most parts of the deformation energy (19) as well as most parts of the work (22) are irreversibly dissipated in crumpling creases such that the amount of accumulated elastic energy is insufficient to initiate the reverse transitions between jammed folding configurations of the crumpling network after the compressive force is withdrawn. Moreover, under increased compression, dynamic rearrangements in crumpling networks of predominantly plastic materials are repressed by plastic deformations (see Refs. [11,13,27]) and so, the relaxation of the compression force and the creep deformation is determined by the energy dissipation in the folding creases rather than by the rearrangement of the energy foci. As a result, the compressive force relaxation and creep in balls that are folded from plastic sheets do not obey evolution equations (15) and (16), rather, they are controlled by another mechanism that is associated with the plastic deformations, which are localized in the crumpling creases. While stretched exponential function (5) provides a good fitting of experimental data on the stress relaxation in hand-folded aluminum foil (see Fig. 6 and Ref. [41]), further experimental and theoretical studies are needed to clarify the mechanisms and functional forms of stress and strain relaxation in randomly crumpled plastic sheets.

V. CONCLUSIONS

To summarize, we found experimentally that, in axially compressed hand crumpled paper, the relaxation of the compressive force under the constant compression ratio and the creep deformation under the constant force follow the relaxation equations (8) and (9), respectively. These equations determine the form of the corresponding equations of evolution (15) and (16), which suggest that the relaxation dynamics in crumpled elastic and elasto-plastic sheets is ruled by activated processes of the rearrangement of the energy foci in the crumpling network, whereas, the stress relaxation in predominantly plastic sheets is controlled by the energy dissipation in the crumpling creases. We pointed out that thermodynamics of activated processes in crumpled sheets can be understood within the framework of Edwards's statistical mechanics. In this way, explicit functional forms of the activation barrier between admissible jammed configurations of the crumpling network under axial compression are derived. Our findings suggest that, under a constant compression ratio, the compressive force decreases due to dissipation and/or redistribution of the deformation energy supplied to the crumpled network during ball compression. On the other hand, under a constant compressive force, the activation barrier between admissible jammed configurations increases as an elastic energy, which is supplied by a compressive

force, is released during creep deformation, which is accompanied by the rearrangement of the energy foci in the crumpling network and energy relaxation in the crumpling creases.

ACKNOWLEDGMENTS

This work was partially supported by the FONCICYT (México-European Union) under Project No. 96095 and the Government of Mexico City under Grant No. PICCT08-38.

[1] M. A. F. Gomes, Am. J. Phys. **55**, 649 (1987); J. B. C. Garcia, M. A. F. Gomes, T. I. Jyh, and T. I. Ren, J. Phys. A **25**, L353 (1992); M. A. F. Gomes, C. C. Donato, S. L. Campello, R. E. de Souza, and R. Cassia-Moura, J. Phys. D: Appl. Phys. **40**, 3665 (2007).

[2] A. Lobkovsky, S. Gentges, H. Li, D. Morse, and T. A. Witten, Science **270**, 1482 (1995).

[3] P. A. Houle and J. P. Sethna, Phys. Rev. E **54**, 278 (1996); D. L. Blair and A. Kudrolli, Phys. Rev. Lett. **94**, 166107 (2005); E. Sultan and A. Boudaoud, *ibid.* **96**, 136103 (2006); D. Aristoff and C. Radin, Europhys. Lett. **91**, 56003 (2010); R. D. Schroll, E. Katifori, and B. Davidovitch, Phys. Rev. Lett. **106**, 074301 (2011); E. Hohlfeld and L. Mahadevan, *ibid.* **106**, 105702 (2011); K. Essafi, J.-P. Kownacki, and D. Mouhanna, *ibid.* **106**, 128102 (2011).

[4] K. Matan, R. B. Williams, T. A. Witten, and S. R. Nagel, Phys. Rev. Lett. **88**, 076101 (2002).

[5] A. S. Balankin, R. C. Montes de Oca, and D. Samayoa, Phys. Rev. E **76**, 032101 (2007); A. S. Balankin, D. Samayoa, I. A. Miguel, J. Patiño, and M. Á. Martínez, *ibid.* **81**, 061126 (2010); A. S. Balankin, S. Matías, D. Samayoa, J. Patiño, B. Espinoza, and C. L. Martínez, *ibid.* **83**, 036310 (2011).

[6] S. Chaieb, V. K. Natrajan, and A. A. El-rahman, Phys. Rev. Lett. **96**, 078101 (2006); V. M. Pereira, A. H. Castro Neto, H. Y. Liang, and L. Mahadevan, *ibid.* **105**, 156603 (2010); E. Prada, P. San-Jose, and L. Brey, *ibid.* **105**, 106802 (2010); T. Tallinen, J. A. Aström, P. Kekäläinen, and J. Timonen, *ibid.* **105**, 026103 (2010).

[7] Y.-C. Lin, J.-M. Sun, J.-H. Hsiao, Y. Hwu, C. L. Wang, and T.-M. Hong, Phys. Rev. Lett. **103**, 263902 (2009); Y.-C. Lin, J.-M. Sun, H. W. Yang, Y. Hwu, C. L. Wang, and T.-M. Hong, Phys. Rev. E **80**, 066114 (2009); W. Bai, Y.-C. Lin, T.-K. Hou, and T.-M. Hong, *ibid.* **82**, 066112 (2010).

[8] Z. Ismat, J. Struct. Geol. **31**, 972 (2009).

[9] T. A. Witten, Rev. Mod. Phys. **79**, 643 (2007).

[10] A. Lobkovsky, Phys. Rev. E **53**, 3750 (1996); G. Gompper, Nature (London) **386**, 439 (1997); E. M. Kramer and T. A. Witten, Phys. Rev. Lett. **78**, 1303 (1997); M. Ben Amar and Y. Pomeau, Proc. R. Soc. London, Ser. A **453**, 729 (1997); E. Cerda and L. Mahadevan, Phys. Rev. Lett. **80**, 2358 (1998); E. Cerda, S. Chaieb, F. Melo, and L. Mahadevan, Nature (London) **401**, 46 (1999); B. A. DiDonna, T. A. Witten, S. C. Venkataramani, and E. M. Kramer, Phys. Rev. E **65**, 016603 (2001); B. A. DiDonna, *ibid.* **66**, 016601 (2002); C. A. Andresen, A. Hansen, and J. Schmittbuhl, *ibid.* **76**, 026108 (2007); T. Tallinen, J. A. Åström, and J. Timonen, Comput. Phys. Commun. **180**, 512 (2009); T. A. Witten, J. Phys. Chem. B **113**, 3738 (2009); T. Tallinen, J. Ojajärvi, J. A. Aström, and J. Timonen, Phys. Rev. Lett. **105**, 066102 (2010).

[11] S. Chaïeb and F. Melo, Phys. Rev. E **60**, 6091 (1999).

[12] B. A. DiDonna and T. A. Witten, Phys. Rev. Lett. **87**, 206105 (2001).

[13] T. Mora and A. Boudaoud, Europhys. Lett. **59**, 41 (2002).

[14] P. Mellado, S. Cheng, and A. Concha, Phys. Rev. E **83**, 036607 (2011).

[15] M. A. F. Gomes, T. I. Jyh, T. I. Ren, I. M. Rodrigues, and C. B. S. Furtado, J. Phys. D: Appl. Phys. **22**, 1217 (1989).

[16] A. S. Balankin and O. Susarrey, Phys. Rev. E **77**, 051124 (2008).

[17] A. S. Balankin *et al.*, Phys. Rev. B **77**, 125421 (2008).

[18] Y. C. Lin, Y. L. Wang, Y. Liu, and T. M. Hong, Phys. Rev. Lett. **101**, 125504 (2008).

[19] I. Dierking and P. Archer, Phys. Rev. E **77**, 051608 (2008).

[20] A. Boudaoud, P. Patrício, Y. Couder, and M. Ben Amar, Nature (London) **407**, 718 (2000).

[21] T. Tallinen, J. A. Aström, and J. Timonen, Phys. Rev. Lett. **101**, 106101 (2008).

[22] H. Aharoni and E. Sharon, Nature Mater. **9**, 993 (2010).

[23] S. F. Edwards and R. B. S. Oakeshott, Physica A **157**, 1080 (1989); S. F. Edwards, in *Granular Matter: An Interdisciplinary Approach*, edited by A. Mehta (Springer-Verlag, New York, 1994); S. F. Edwards and D. V. Grinev, Adv. Phys. **51**, 1669 (2002).

[24] A. Barrat, J. Kurchan, V. Loreto, and M. Sellitto, Phys. Rev. Lett. **85**, 5034 (2000); A. Barrat, J. Kurchan, V. Loreto, and M. Sellitto, Phys. Rev. E **63**, 051301 (2001); A. Fierro, M. Nicodemi, and A. Coniglio, *ibid.* **66**, 061301 (2002); M. Schröter, D. I. Goldman, and H. L. Swinney, *ibid.* **71**, 030301(R) (2005); M. P. Ciamarra, A. Coniglio, and M. Nicodemi, Phys. Rev. Lett. **97**, 158001 (2006).

[25] S. Deboeuf, M. Adda-Bedia, and A. Boudaoud, Europhys. Lett. **85**, 24002 (2009); M. Adda-Bedia, A. Boudaoud, L. Boué, and S. Deboeuf, J. Stat. Mech.: Theory Exp. (2010) P11027.

[26] G. A. Vliegenthart and G. Gompper, Nature Mat. **5**, 216 (2006).

[27] T. Tallinen, J. A. Aström, and J. Timonen, Nature Mater. **8**, 25 (2009).

[28] A. S. Balankin, D. Morales, E. Pineda, A. Horta, M. Á. Martínez, and D. Samayoa, Physica A **388**, 1780 (2009).

[29] A. S. Balankin, O. Susarrey, R. Cortes, D. Samayoa, J. Martínez, and M. A. Mendoza, Phys. Rev. E **74**, 061602 (2006).

[30] A. S. Balankin, I. Campos, O. A. Martínez, and O. Susarrey, Phys. Rev. E **75**, 051117 (2007).

[31] M. Davis and N. Thompson, Proc. Phys. Soc. London, Sect. B **63**, 847 (1950); A. H. Cottrell, J. Mech. Phys. Solids **1**, 53 (1952); N. F. Mott, Philos. Mag. **44**, 742 (1953); O. H. Wyatt, Proc. Phys. Soc. London, Sect. B **66**, 459 (1953); G. C. E. Olds, *ibid.* **67**, 832 (1954).

[32] R. W. K. Honeycombe, *The Plastic Deformation of Metals*, 2nd ed., Chap. 13 (Arnold, London, 1984).

[33] F. R. N. Nabarro, Mater. Sci. Eng. A **309-310**, 227 (2001).

[34] H. W. Haslach Jr., Mech. Time-Depend. Mater. **4**, 169 (2000).

[35] G. I. Taylor, Proc R. Soc. London, Ser. A **145**, 362 (1934).
[36] P. Hähner, A. Ziegenbein, E. Rizzi, and H. Neuhäuser, Phys. Rev. B **65**, 134109 (2002).
[37] U. F. Kocks and H. Mecking, Prog. Mater. Sci. **48**, 171 (2003).
[38] G. Ananthakrishna, Phys. Rep. **440**, 113 (2007).
[39] G. Debrégeas, H. Tabuteau, and J.-M. di Meglio, Phys. Rev. Lett. **87**, 178305 (2001); J.-B. Salmon, S. Manneville, and A. Colin, Phys. Rev. E **68**, 051504 (2003); R. P. Behringer, D. Bi, B. Chakraborty, S. Henkes, and R. R. Hartley, Phys. Rev. Lett. **101**, 268301 (2008); L. Bocquet, A. Colin, and A. Ajdari, *ibid.* **103**, 036001 (2009); A. Lemaître and C. Caroli, *ibid.* **103**, 065501 (2009).
[40] K. A. Reddy, Y. Forterre, and O. Pouliquen, Phys. Rev. Lett. **106**, 108301 (2011).
[41] R. F. Albuquerque and M. A. F. Gomes, Physica A **310**, 377 (2002).
[42] K. P. Mota and P. M. C. de Oliveira, Physica A **387**, 6095 (2008).
[43] M. Alava and K. Niskanen, Rep. Prog. Phys. **69**, 669 (2006).
[44] In some experiments performed in the climatic chamber, we observed the stain relaxation under a fixed force for up to 35 days.
[45] Notice that, in the experiments performed in Ref. [4], the weight piston was slightly lifted and was fixed in place such that it could no longer compress the material, whereas, in our experiments, the plate was not lifted before its position was fixed. Moreover, the lateral dimensions of the compressed sheets were confined, whereas, in our experiments, the lateral dimensions were free.
[46] In this paper, while we presented comparisons of data fittings with only a few different functions, more fitting functions were tested to find the best fit.
[47] A. Gurevich and H. Küpfer, Phys. Rev. B **48**, 6477 (1993); J. J. Brey and A. Prados, Phys. Rev. E **63**, 021108 (2001); R. Hilfer, *ibid.* **65**, 061510 (2002); N. W. Tschoegl, W. G. Knauss, and I. Emri, Mech. Time-Depend. Mater. **6**, 3 (2002); R. Metzlera and T. F. Nonnenmacher, Int. J. Plast. **19**, 941 (2003); V. Desoutter and N. Destainville, Eur. Phys. J. B **37**, 383 (2004); F. Brouers and O. Sotolongo-Costa, Physica A **356**, 359 (2005); **368**, 165 (2006); J. Bursa and P. Janícek, J. Eng. Mech. **16**, 335 (2009).
[48] We noted that τ_F decreased as the humidity or temperature increased; in our experiments, the value of τ_F was varied in the range of $0.1 \leqslant \tau_F \leqslant 40$ s for Kraft and $2 \leqslant \tau_F \leqslant 70$ s for Biblia papers. It is interesting to note that, according to Eq. (7), an axially compressed ball can only achieve a steady state $dF/dt = 0$ when $F = 0$ after $T = \tau[\exp(\beta^{-1}) - 1] \approx 10^4$ years.
[49] Without external restrictions, an elastic sheet unfolds to a plane state.
[50] P. Chauve, T. Giamarchi, and P. Le Doussal, Phys. Rev. B **62**, 6241 (2000).